

Prediction of CO₂ storage with Enhanced Natural Gas Recovery Based on Backpropagation Neural Network

Honglue Huang¹, Shuyang Liu^{1,2*}, Junrong Liu¹, Zhiqiang Wang¹

1 School of Petroleum Engineering, China University of Petroleum (East China), Qingdao 266580, Shandong, P.R. China

2. Key Laboratory of Intelligent Construction and Health Monitoring for Deep Underground Engineering, Shenzhen University, Nanshan District, Shenzhen 518060, P.R. China

(*Corresponding Author: shuyang_liu@126.com)

ABSTRACT

CO₂ storage with enhanced gas recovery (CSEGR) offers the dual benefits of boosting natural gas production while achieving effective carbon sequestration, presenting broad prospects for industrial application. In this study, a numerical model of CSEGR was constructed using geological data from the Dongfang 1-1 gas field in the South China Sea to assess how different injection–production schemes and reservoir conditions affect both gas recovery and CO₂ storage. To further enhance predictive capabilities, a backpropagation (BP) neural network–based surrogate model was developed. The AI-driven model accurately captured the nonlinear relationships between geological and engineering parameters and the performance outcomes. Results show that gas recovery increases with CO₂ injection rate and permeability, while decreasing with bottomhole pressure and porosity. Conversely, CO₂ storage performance improves with higher injection rates and bottomhole pressures but declines with greater permeability and porosity. The BP neural network achieved an average prediction accuracy of 95%, highlighting its effectiveness as a reliable tool for forecasting CSEGR performance under complex reservoir conditions.

Keywords: CCUS, CO₂ enhanced gas recovery, CO₂ storage, BP neural network

1. INTRODUCTION

Global climate change and environmental issues have become increasingly severe. In response to this challenge, China formally proposed its goals of carbon peaking and carbon neutrality at the 75th United Nations General Assembly in September 2020, aiming to peak carbon dioxide emissions before 2030 and achieve

carbon neutrality by 2060^[1,2,3]. Under the constraints of these goals, natural gas, as a low-carbon and clean energy source, plays a crucial role as a transitional bridge in the shift from high- carbon to zero-carbon energy systems^[4].

Carbon Capture, Utilization, and Storage (CCUS) is a comprehensive technology widely regarded as one of the most effective strategies for mitigating global warming^[5]. It involves capturing CO₂ from industrial emission sources and subsequently utilizing or storing it to reduce atmospheric CO₂ levels, thereby slowing climate change. CSEGR is a key application of CCUS in the oil and gas sector, enabling both the improvement of natural gas recovery and the geological sequestration of CO₂. The widespread implementation of CSEGR contributes not only to enhancing global natural gas production and alleviating current limitations in supply capacity, but also to reducing CO₂ emissions, thereby playing a significant role in advancing global carbon neutrality and climate mitigation objectives.

Compared with depleted oil reservoirs, depleted gas reservoirs offer greater CO₂ storage potential^[6]. Their geological structures typically exhibit excellent sealing and injectivity^[7], and the availability of well-established infrastructure and detailed geological data from previous gas production operations^[8] further supports large-scale CO₂ injection. Additionally, due to the long-term containment of natural gas over hundreds of years, these reservoirs possess substantial potential for long-term CO₂ storage^[9]. Injecting CO₂ into such reservoirs not only supports stable long-term storage but also yields economic benefits through CSEGR^[10].

At present, injection parameters (e.g., gas type, injection timing, and injection rate) and geological parameters (e.g., porosity and permeability) are recognized as critical factors influencing CO₂ migration

behavior and optimal injection–production strategies in CSEGR and sequestration assessments [11,12,13]. However, existing studies tend to focus on specific aspects, with limited consideration of the comprehensive interplay among these factors.

In recent years, with the rapid advancement of artificial intelligence (AI), its applications in the petroleum industry have become increasingly widespread, particularly in areas such as reservoir numerical simulation, injection–production scheme optimization, and production forecasting, where it has demonstrated significant advantages [14]. Polak et al. [15] conducted a simulation study on the potential of CSEGR in the depleted Atzbach–Schwanenstadt gas reservoir in Austria. Using the Eclipse 300 compositional simulator, they constructed a 3D geological model and analyzed four different gas injection scenarios. The results showed that up to 8.2 Mt of CO₂ could be stored over a 30-year injection period. Kashkooli et al. [16] proposed a coupled optimization model aimed at maximizing both hydrocarbon recovery and CO₂ storage efficiency. By introducing genetic algorithms and pattern search methods to regulate bottomhole pressure as an optimization variable, the final optimized scheme improved CO₂ storage efficiency by 12.1% and increased the overall objective function by 2.86%.

Among various AI algorithms, the backpropagation (BP) neural network [17] is one of the most widely used and mature approaches in oilfield applications. It is a multilayer feedforward neural network that follows the principle of error backpropagation. The network architecture consists of an input layer, at least one hidden layer, and an output layer, with full inter-layer connectivity between neurons, but no lateral or cross-layer feedback connections, forming a strictly hierarchical information processing system [18]. Based on this foundation, this study adopts CMG numerical simulation software to construct a CSEGR model using geological and fluid property data from the Dongfang 1-1 gas field in the South China Sea. First, the effects of typical injection–production and reservoir parameters on gas recovery, CO₂ storage volume, and storage efficiency are analyzed. Subsequently, an expanded set of parameters is used to train a BP neural network to accurately predict gas recovery and CO₂ sequestration performance. This approach provides both theoretical insights and practical guidance for the application of CSEGR and integrated carbon storage in real gas reservoirs.

2. METHODOLOGY

2.1 Numerical model of CSEGR

A numerical model for CSEGR was developed based on the geological characteristics of the Upper Reservoir III in the Dongfang 1-1 gas field, located in the northern South China Sea. The porosity of the target reservoir ranges from 14% to 30%, with a median value of 22%. Permeability varies from 0.3 to $160 \times 10^{-3} \mu\text{m}^2$, with a median of $13 \times 10^{-3} \mu\text{m}^2$. Well test data indicate a vertical-to-radial permeability ratio (K_z/K_r) of 0.044, corresponding to a vertical permeability of $0.572 \times 10^{-3} \mu\text{m}^2$ [19,20].

As shown in Fig.1, A five-spot well pattern was employed, and a homogeneous reservoir model was constructed using one-quarter of the pattern configuration. Numerical simulations were conducted using the CMG simulator. The model dimensions in the X and Y directions are 2100 m each, with a thickness of 35 m in the Z direction. The grid size is 55 m × 55 m × 1 m, resulting in 39 × 39 × 35 grid blocks and a total of 53,235 cells. The reservoir top is located at a depth of 1350 m, with a geothermal gradient of 4.67 °C per 100 m. Under these conditions, the temperature and pressure at the top of the reservoir are 81.5 °C and 14.08 MPa, respectively.

The injection well is positioned in the lower-left corner of the model, while the production well is located in the upper-right corner and extends to the base of the reservoir. Both wells are fully perforated across the entire reservoir thickness. The minimum production rate for the production well is set at 40,000 standard cubic meters per day; if the rate falls below this threshold, the well is shut in. The primary components considered in the simulation are CH₄, CO₂, and N₂, with molar ratios of 0.511:0.336:0.153, respectively, based on field data [21,22].

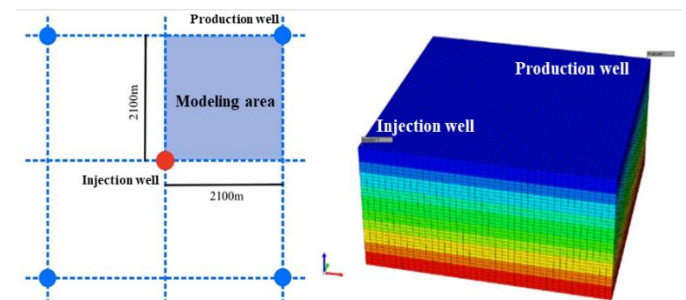


Fig. 1. Schematic diagram of CSEGR model

2.2 The construction of BP neural network

A simplified schematic of the neural network architecture is presented in Fig.2, the BP neural network

constructed in this study consists of an input layer (10 features), three hidden layers (with 128, 256, and 64 neurons, respectively), and an output layer (4 target variables). A dynamic learning rate strategy (initially 0.01, reduced to below 1×10^{-6} and weight decay (1×10^{-4}) were employed, along with early stopping to enhance generalization. Mean Squared Error (MSE) was used as the loss function, and ReLU was adopted as the activation function. All input features were normalized via linear transformation, and outputs were rescaled using inverse transformation.

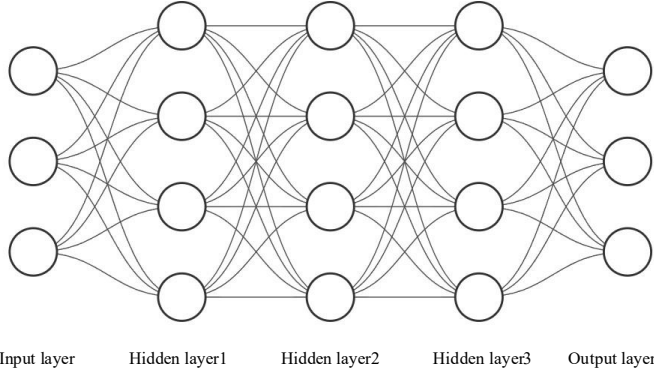


Fig. 2. Simplified architecture of the neural network

In the previous analysis, the effects of certain injection–production parameters and reservoir properties on natural gas recovery, CO₂ storage capacity, and storage efficiency have been considered. To further enhance the comprehensiveness of the evaluation, ten parameters were incorporated into the analysis, including: CO₂ injection rate ν , bottom-hole pressure of the production well BHP , duration of natural depletion t_1 , duration of CO₂-enhanced gas recovery t_2 , fracture pressure of the reservoir P_f , horizontal permeability k , daily gas production constraint per well q , formation temperature at 1450 m T_f , vertical permeability k_z , and porosity φ . The value ranges for these parameters are summarized in Table 1.

The Latin Hypercube Design (LHD) method was employed to generate parameter combinations, ensuring comprehensive coverage of the possible parameter space and thereby enhancing the accuracy and robustness of the predictive results. These parameter combinations were then input into the CSEGR simulation model to obtain a dataset consisting of 792 samples. The dataset was subsequently divided into training, validation, and testing, which were used to train, validate, and test the performance of the backpropagation (BP) neural network.

Table1 The value range of each parameter

Parameter	Value Range
$\nu /(\text{m}^3 \cdot \text{d}^{-1})$	40000-120000
BHP / MPa	1.5-4.5
t_1 / year	6-18
t_2 / year	40-60
P_f / MPa	17.04-36.05
$k / (10^{-3} \mu\text{m}^2)$	10-100
$q / (\text{m}^3 \cdot \text{d}^{-1})$	30000-50000
$T_f / ^\circ\text{C}$	82.5-87.5
$k_z / (10^{-3} \mu\text{m}^2)$	0.3-30
φ	0.15-0.4

3. RESULTS AND DISCUSSIONS

3.1 Numerical simulation of CSEGR

Based on the CSEGR numerical model, a series of sensitivity analyses were conducted by varying injection and production parameters, as well as reservoir properties, to evaluate system responses under different geological and operational conditions. The dynamics of gas production were assessed through key performance indicators, including natural gas recovery factor, CO₂ sequestration efficiency, and total CO₂ storage volume. These analyses aim to identify the critical parameters that govern the effectiveness of CO₂-enhanced natural gas recovery and associated carbon sequestration performance.

3.1.1 Effect of CO₂ injection rate

As shown in Fig.3, the natural gas recovery factor, CO₂ storage volume, and CO₂ sequestration efficiency all increase with the CO₂ injection rate. This is primarily because a higher injection rate leads to a greater total volume of CO₂ injected into the reservoir, thereby enhancing the potential for underground CO₂ storage. At the same time, the elevated injection rate increases reservoir pressure, providing stronger displacement energy for CH₄ and resulting in improved gas recovery.

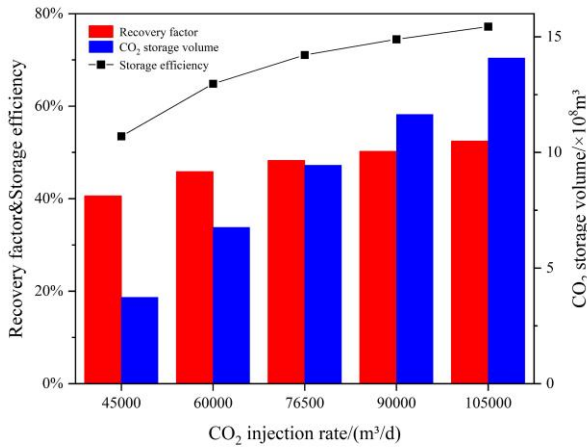


Fig. 3. Effect of CO₂ injection rate on recovery, storage volume, and storage efficiency

Furthermore, as shown in fig.4, the daily gas production rate and production duration are significantly influenced by the CO₂ injection rate. It can be observed that the single-well daily production rate increases with injection rate. At an injection rate of 45,000 m³·d⁻¹, the well was shut in after 20,708 days of production due to the daily output falling below the economic threshold of 50,000 m³. Consequently, higher injection rates help sustain elevated daily gas production levels, thereby improving the economic viability of CSEGR operations.

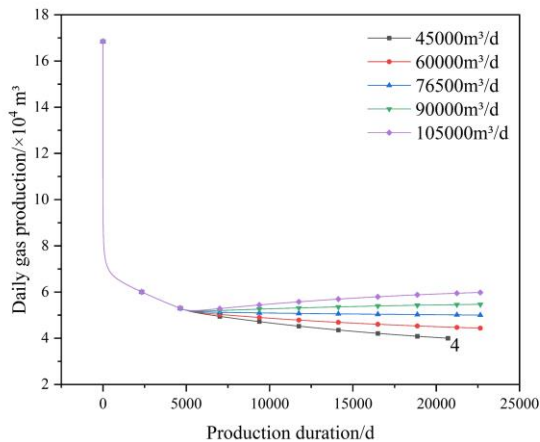


Fig. 4. Variation of daily gas production at different CO₂ injection rates

3.1.2 Effect of Production well bottom-hole pressure

As shown in Fig. 5, the natural gas recovery factor increases with decreasing bottom-hole pressure (BHP) at the production well. Conversely, both the CO₂ storage volume and sequestration efficiency decrease as the bottom-hole pressure declines.

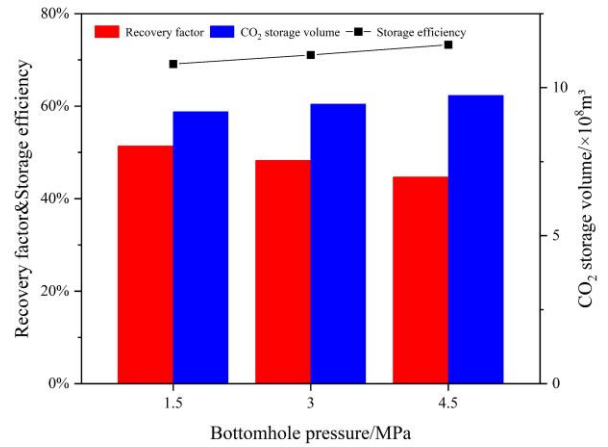


Fig. 5. Effect of bottom-hole pressure on recovery efficiency, CO₂ storage volume, and storage efficiency

As illustrated in Fig.6, with increasing BHP at the production well, the gas production resistance rises, leading to a reduction in daily gas production per well and a subsequent decrease in natural gas recovery. Under fixed CO₂ injection rate and injection duration, the amount of produced CO₂ decreases, resulting in an increase in both CO₂ storage volume and sequestration efficiency.

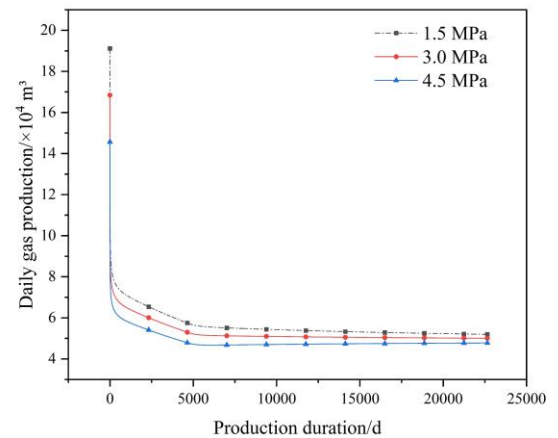


Fig. 6. Daily gas production variation under different bottomhole pressures

3.1.3 Effect of Porosity

As shown in Fig.7, the natural gas recovery factor, CO₂ storage volume, and sequestration efficiency all decrease with increasing reservoir porosity.

When the reservoir porosity is 0.15, the natural gas recovery factor reaches 66.24%, representing an 18% increase compared to the baseline case. The corresponding CO₂ storage volume is 9.65×10^8 m³,

which is $2 \times 10^7 \text{ m}^3$ higher than the baseline, while the sequestration efficiency decreases by 1.54%. At a porosity of 0.3, the natural gas recovery factor decreases by 11.15% relative to the baseline, the CO₂ storage volume declines by $1.9 \times 10^7 \text{ m}^3$, and sequestration efficiency improves by 1.35%.

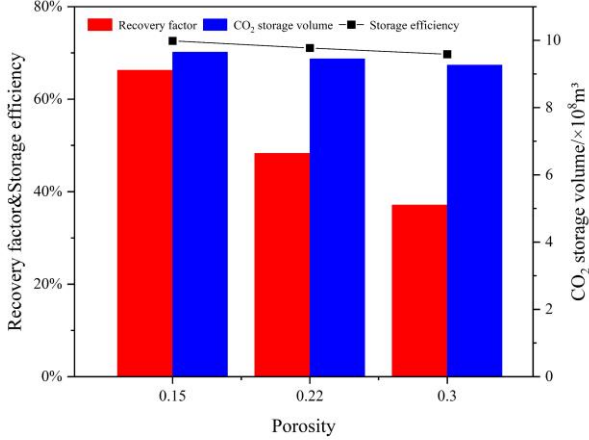


Fig. 7. Effect of porosity on natural gas recovery, CO₂ storage volume, and storage efficiency

Fig.8 indicates that the actual CH₄ production volume increases with porosity. Under the condition where only porosity varies and the gas composition remains constant, the original gas in place (OGIP) also increases with porosity, resulting in a decline in recovery factor, as shown in fig.9. Meanwhile, the amount of produced CO₂ increases, but since the CO₂ injection rate and injection duration are unchanged, the total amount of CO₂ injected into the reservoir remains constant, leading to a decrease in both CO₂ storage volume and sequestration efficiency.

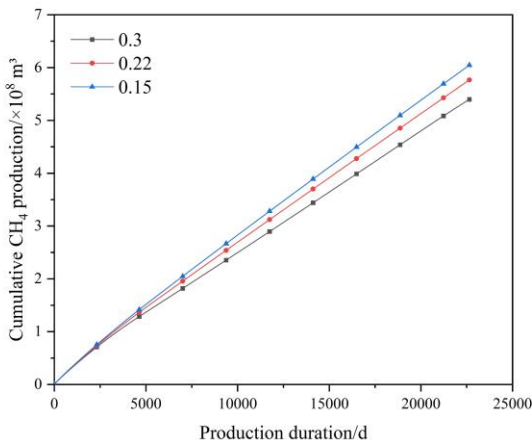


Fig. 8. The variation of CH₄ production with different porosity

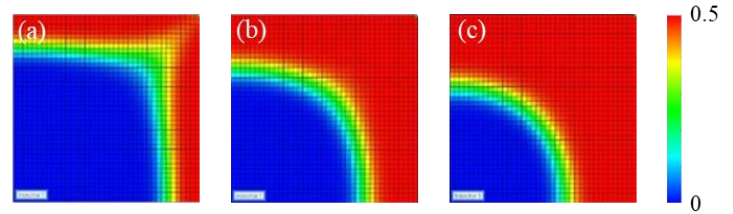


Fig. 9. Final CH₄ saturation distribution under different porosity

3.1.4 Effect of Permeability

As illustrated in Fig.10, the natural gas recovery factor increases with increasing permeability, while both the CO₂ storage volume and sequestration efficiency decrease as permeability rises. When the permeability reaches $53 \times 10^{-3} \mu\text{m}^2$, the natural gas recovery factor increases by 34.51% compared to the baseline case, whereas the CO₂ storage volume decreases by $4.07 \times 10^8 \text{ m}^3$ and sequestration efficiency declines by 30.57%. At a permeability of $93 \times 10^{-3} \mu\text{m}^2$, the recovery factor further increases by 38.37%, with the CO₂ storage volume reduced by $6.19 \times 10^8 \text{ m}^3$ and sequestration efficiency dropping by 46.53%.

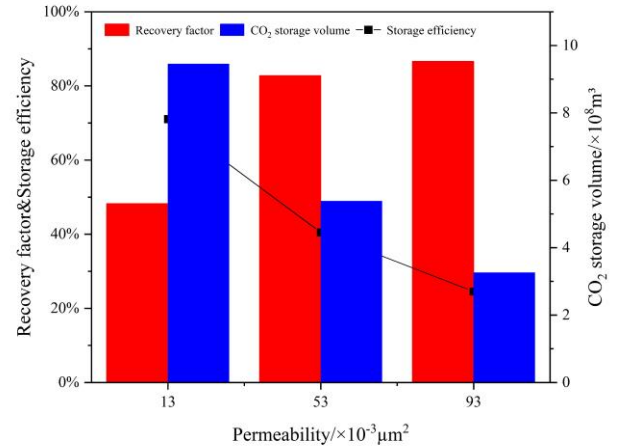


Fig. 10. Effect of permeability on natural gas recovery, CO₂ storage volume, and storage efficiency

The increase in permeability leads to a significant rise in CO₂ production, resulting in a substantial reduction in both CO₂ storage volume and sequestration efficiency, as shown in fig.11. Concurrently, as permeability increases, CH₄ previously uncontacted around the production well is effectively displaced, markedly improving sweep efficiency and thus significantly enhancing gas recovery.

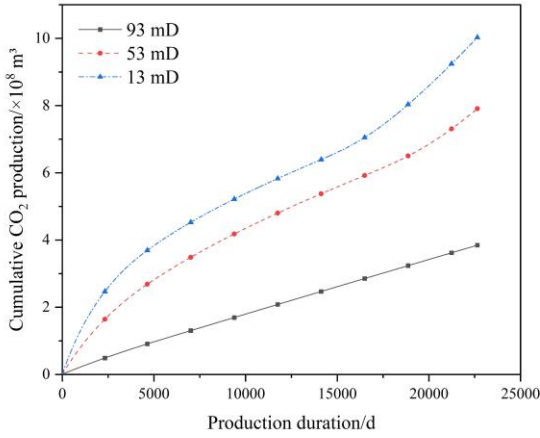


Fig. 11. CO₂ production under different permeability

3.2 Prediction based on BP neural network model

The constructed BP neural network was employed to predict the cumulative gas production, cumulative CH₄ production, cumulative CO₂ injection, and cumulative CO₂ production, corresponding to Fig.12 (a), (b), (c), and (d), respectively. The mean prediction errors for these four outputs were 3.67%, 3.66%, 5.06%, and 4.28%, respectively.

The relative prediction deviation of the constructed BP neural network are shown in Fig.13. With the input layer incorporating 10 input parameters, the model demonstrates generally low errors in predicting cumulative gas production, cumulative CH₄ production, cumulative CO₂ injection, and cumulative CO₂ production. As illustrated in Fig.13, the highest prediction accuracy is achieved for cumulative CO₂ injection.

These results demonstrate that the BP neural network developed in this study exhibits strong predictive performance in estimating the outcomes of CSEGR. The model effectively captures complex nonlinear relationships and shows good adaptability to variations in injection–production parameters and

reservoir properties. This provides a solid foundation for the subsequent integration with optimization algorithms to achieve parameter optimization.

4. CONCLUSIONS

1. A numerical simulation model of CO₂ storage with enhanced gas recovery (CSEGR) was developed, incorporating both injection–production parameters and reservoir characteristics to evaluate their combined effects on gas recovery and CO₂ storage performance.

2. Considering reservoir properties and economic feasibility, natural gas recovery is positively correlated with CO₂ injection rate, depletion time, permeability, and reservoir dip angle, and negatively correlated with bottomhole pressure and porosity. CO₂ storage volume and storage efficiency exhibit positive correlations with CO₂ injection rate, bottomhole pressure, and dip angle, and negative correlations with depletion time, permeability, and porosity. A lower formation fracture pressure imposes stronger constraints on gas recovery, CO₂ storage volume, and storage efficiency.

3. The backpropagation (BP) neural network shows strong capability in capturing nonlinear relationships and achieves high prediction accuracy for gas recovery, CO₂ storage volume, and storage efficiency under varying injection–production and reservoir parameters, making it a promising AI-based approach for CSEGR performance forecasting.

ACKNOWLEDGEMENT

This paper has been financially supported by the National Natural Science Foundation of China (52374063 and 52204065), and Shandong Provincial Natural Science Foundation (ZR2023ME049), the Fundamental Research Funds for the Central Universities (25CX07004A), which are gratefully acknowledged.

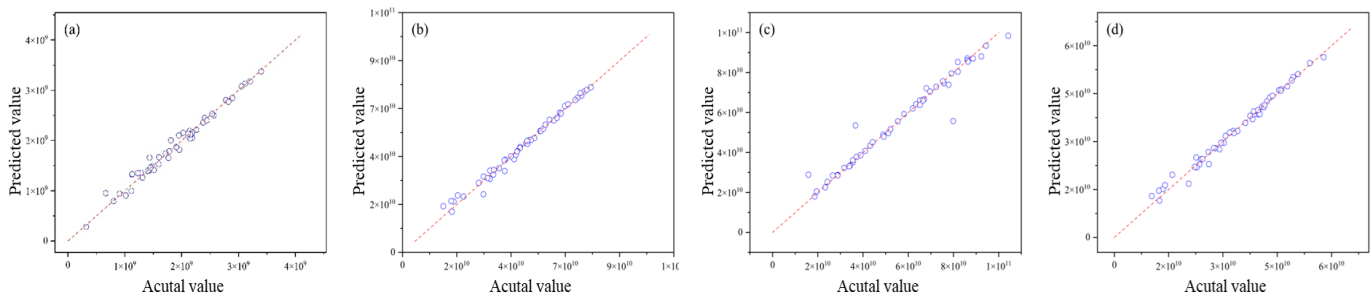


Fig. 12. Graph comparing predicted and actual values

DECLARATION OF INTEREST STATEMENT

The authors declare that they have no known competing financial interests or personal relationships that could have appeared to influence the work reported in this paper. All authors read and approved the final manuscript.

aspects and economics[J]. *Geoenergy Science and Engineering*, 2024: 212726.

[6] Mamora D D, Seo J G. Enhanced gas recovery by carbon dioxide sequestration in depleted gas reservoirs[C]//SPE Annual Technical Conference and Exhibition?. SPE, 2002: SPE-77347-MS.

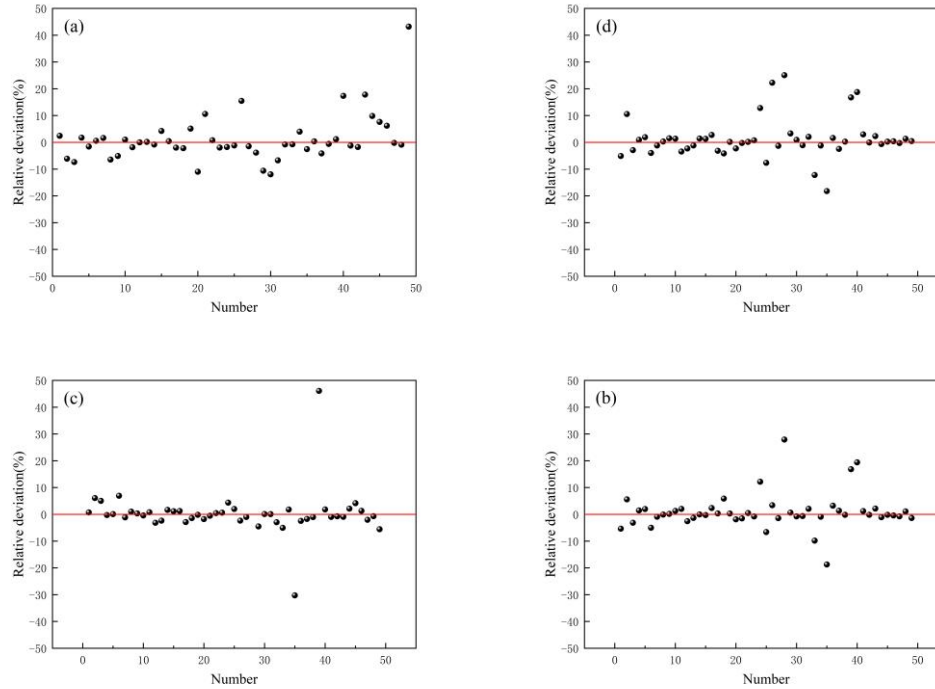


Fig. 13. The relative deviation of BP neural network

REFERENCE

- [1] Jiang Q, Yin Z. The optimal path for China to achieve the “Dual Carbon” target from the perspective of energy structure optimization[J]. *Sustainability*, 2023, 15(13): 10305.
- [2] China Government Network. Xi Jinping attended the general debate of the 76th UN General Assembly and delivered an important speech. Sept. 2021. http://www.gov.cn/xinwen/2021-09/22/content_5638596.htm.
- [3] Shi X, Zheng Y, Lei Y, et al. Air quality benefits of achieving carbon neutrality in China[J]. *Science of the Total Environment*, 2021, 795: 148784.
- [4] Zou C N, Xue H Q, Xiong B, et al. Connotation, innovation, and vision of "carbon neutrality" [J]. *Natural Gas Industry*, 2021, 41(8): 46–57. (in Chinese)
- [5] Nath F, Mahmood M N, Yousuf N. Recent advances in CCUS: A critical review on technologies, regulatory

[7] Li B Z, Tian X F, Tang E G, et al. Assessment and prospects of CO₂ storage potential in typical depleted gas reservoirs in the South China Sea [J]. *Natural Gas Exploration and Development*, 2024, 47(6): 116–121. (in Chinese)

[8] Metz B, Davidson O, De Coninck H C, et al. IPCC special report on carbon dioxide capture and storage[M]. Cambridge: Cambridge University Press, 2005.

[9] Kubus P. CCS and CO₂-storage possibilities in Hungary[C]//SPE International Conference on CO₂ Capture, Storage, and Utilization. SPE, 2010: SPE-139555-MS.

[10] Zhang L H, Xiong W, Zhao Y L, et al. Mechanism of enhanced gas recovery and CO₂ sequestration by CO₂ injection into depleted bottom-water gas reservoirs [J]. *Natural Gas Industry*, 2024, 44(4). (in Chinese)

[11] Zhang L H, Cao C, Wen S M, et al. Reflections on the development of CO₂-EGR under the background of carbon peaking and carbon neutrality [J]. *Natural Gas Industry*, 2023, 43(1): 13–22. (in Chinese)

- [12] Hamza A, Hussein I A, Al-Marri M J, et al. CO₂ enhanced gas recovery and sequestration in depleted gas reservoirs: A review[J]. *Journal of Petroleum Science and Engineering*, 2021, 196: 107685.
- [13] Sim S S K, Turtata A T, Singhal A K, et al. Enhanced gas recovery: Factors affecting gas-gas displacement efficiency[J]. *Journal of Canadian Petroleum Technology*, 2009, 48(08): 49-55.
- [14] Wang T, Wei Q, **ong W, et al. Current status and prospects of artificial intelligence technology application in oil and gas field development[J]. *ACS omega*, 2024, 9(3): 3173-3183.
- [15] Polak S, Grimstad A A. Reservoir simulation study of CO₂ storage and CO₂-EGR in the Atzbach–Schwanenstadt gas field in Austria[J]. *Energy procedia*, 2009, 1(1): 2961-2968.
- [16] Kashkooli S B, Gandomkar A, Riazi M, et al. Coupled optimization of carbon dioxide sequestration and CO₂ enhanced oil recovery[J]. *Journal of Petroleum Science and Engineering*, 2022, 208: 109257.
- [17] Li H, Yu H, Cao N, et al. Applications of artificial intelligence in oil and gas development[J]. *Archives of Computational Methods in Engineering*, 2021, 28: 937-949.
- [18] Buscema M. Back propagation neural networks[J]. *Substance use & misuse*, 1998, 33(2): 233-270.
- [19] Tong C X, Wang Z F, Li X S. Accumulation conditions and geological implications of the Dongfang 1-1 gas field in the Yinggehai Basin [J]. *Natural Gas Industry*, 2012, 32(8): 11–15, 26, 126. (in Chinese)
- [20] Wang Y C, Liu P, Li G L, et al. Formation water characteristics and their relationship with hydrocarbon preservation in the Dongfang 1-1 gas field, Yinggehai Basin [J]. *Natural Gas Exploration and Development*, 2010, 33(2): 19–22, 6. (in Chinese)
- [21] Zhang L, Ren S R, Wang R H, et al. Feasibility study on CO₂ sequestration in saline aquifers associated with CO₂-rich gas at the Dongfang 1-1 gas field [J]. *Journal of China University of Petroleum (Natural Science Edition)*, 2010, 34(3): 89–93. (in Chinese)
- [22] Jiang P, He W, Cheng T. Economic and efficient development practice and insights of the Dongfang 1-1 gas field [J]. *Natural Gas Industry*, 2012, 32(8): 16–21, 126–127. (in Chinese)